Anal. Chem. **2008,** *80,* 3890–3896

Development of Quantitative Cell-Based Enzyme Assays in Microdroplets

Ansgar Huebner,[†,‡,§] Luis F. Olguin,[†,‡,§] Daniel Bratton,[∥] Graeme Whyte,[∥] Wilhelm T. S. Huck,[∥] Andrew J. de Mello,[⊥] Joshua B. Edel,[⊥,#] Chris Abell,[*,‡] and Florian Hollfelder[*,†]

Department of Biochemistry, University of Cambridge, 80 Tennis Court Road, Cambridge, CB2 1GA, U.K., Department of Chemistry, University of Cambridge, The University Chemical Laboratory, Lensfield Road, Cambridge, CB2 1EW, U.K., Melville Laboratory for Polymer Synthesis, Department of Chemistry, University of Cambridge, The University Chemical Laboratory, Lensfield Road, Cambridge, CB2 1EW, U.K., and Institute of Biomedical Engineering and Department of Chemistry, Imperial College London, South Kensington, London, SW7 2AZ, U.K.

We describe the development of an enzyme assay inside picoliter microdroplets. The enzyme alkaline phosphatase is expressed in *Escherichia coli* cells and presented in the periplasm. Droplets act as discrete reactors which retain and localize any reaction product. The catalytic turnover of the substrate is measured in individual droplets by monitoring the fluorescence at several time points within the device and exhibits kinetic behavior similar to that observed in bulk solution. Studies on wild type and a mutant enzyme successfully demonstrated the feasibility of using microfluidic droplets to provide time-resolved kinetic measurements.

The development of microfluidic microdroplets has provided a new experimental format for biology, and in particular for assay development. The use of pico- to nanoliter scale droplets separated in a moving oil stream compartmentalizes individual reactions. These droplets can be easily manipulated, for example methods have been described for droplet incubation,[1–3] splitting,[4] fusion,[5–7] sorting,[6,8–10] cooling,[11] and heating.[12] These unit operations essentially provide the components of a toolkit which could be used for a future platform technology that relies on integration of these modules.

Among the biochemical tasks that have been studied using microdroplets are *in vitro* protein expression,[1,3] enzymatic assays,[13–15] protein crystallization,[16,17] DNA binding assays[18] and detection of protein expression in cells.[19] Importantly, the compartmentalization provided by droplets is particularly valuable for the detection of enzyme catalytic turnover, not least because a discrete volume element avoids diffusion of the product and allows reliable measurement of its concentration.

For enzyme assays, the enzyme can be delivered as a reagent, but can also be produced *in situ* by cells. Cell-based assays are used in cell biology[20,21] and as part of screening cascades in drug discovery.[22] They are also a key step in directed evolution of catalytic proteins where the colocalization of genotype (i.e., the nucleic acid encoding a potential catalyst) and phenotype (i.e., a functional trait, namely product formation) provides the basis for selecting active catalysts from a library of mutants.[23] Encapsulation of cells in water-in-oil-in-water double emulsion droplets has been a new format for directed evolution studies of several hydrolytic enzymes in which selection from bulk emulsions was achieved by fluorescence-activated cell sorting (FACS) based on end-point measurement of product formation.[24,25] In these experiments the

* Corresponding authors. E-mail: fh111@cam.ac.uk; ca26@cam.ac.uk. Tel: int-44-1223-766048. Fax: int-44-1223-766002.
† Department of Biochemistry, University of Cambridge.
‡ Department of Chemistry, University of Cambridge.
§ Authors contributed equally.
∥ Melville Laboratory for Polymer Synthesis, Department of Chemistry, University of Cambridge.
⊥ Department of Chemistry, Imperial College London.
Institute of Biomedical Engineering, Imperial College London.

(1) Courtois, F.; Olguin, L.; Whyte, G.; Bratton, D.; Huck, W.; Abell, C.; Hollfelder, F. *ChemBioChem* **2008**, *9*, 439–446.
(2) Song, H.; Tice, J. D.; Ismagilov, R. F. *Angew. Chem., Int. Ed.* **2003**, *42*, 768–772.
(3) Dittrich, P. S.; Jahnz, M.; Schwille, P. *ChemBioChem* **2005**, *6*, 811–814.
(4) Link, D. R.; Anna, S. L.; Weitz, D. A.; Stone, H. A. *Phys. Rev. Lett.* **2004**, *92*, 054503.
(5) Fidalgo, L. M.; Abell, C.; Huck, W. T. S. *Lab Chip* **2007**.
(6) Link, D. R.; Grasland-Mongrain, E.; Duri, A.; Sarrazin, F.; Cheng, Z.; Cristobal, G.; Marquez, M.; Weitz, D. A. *Angew. Chem., Int. Ed.* **2006**, *45*, 2556–2560.
(7) Baroud, C. N.; Vincent, M. R. d. S.; Delville, J.-P. *Lab Chip* **2007**.
(8) Ahn, K.; Agresti, J.; Chong, H.; Marquez, M.; Weitz, D. A. *Appl. Phys. Lett.* **2006**, *88*, 264105–264103.
(9) Joanicot, M.; Ajdari, A. *Science* **2005**, *309*, 887–888.
(10) Fidalgo, L. M.; Whyte, G.; Bratton, D.; Kaminski, C. F.; Abell, C.; Huck, W. T. *Angew. Chem., Int. Ed.* **2008**, *47*, 2042–2045.
(11) Sgro, A. E.; Allen, P. B.; Chiu, D. T. *Anal. Chem.* **2007**, *79*, 4845–4851.
(12) Chan, E. M.; Alivisatos, A. P.; Mathies, R. A. *J. Am. Chem. Soc.* **2005**, *127*, 13854–13861.
(13) Roach, L. S.; Song, H.; Ismagilov, R. F. *Anal. Chem.* **2005**, *77*, 785–796.
(14) Song, H.; Ismagilov, R. F. *J. Am. Chem. Soc.* **2003**, *125*, 14613–14619.
(15) Song, H.; Li, H. W.; Munson, M. S.; Van Ha, T. G.; Ismagilov, R. F. *Anal. Chem.* **2006**, *78*, 4839–4849.
(16) Zheng, B.; Gerdts, C. J.; Ismagilov, R. F. *Curr. Opin. Struct. Biol.* **2005**, *15*, 548–555.
(17) Zheng, B.; Tice, J. D.; Ismagilov, R. F. *Anal. Chem.* **2004**, *76*, 4977–4982.
(18) Srisa-Art, M.; deMello, A. J.; Edel, J. B. *Anal. Chem.* **2007**, *79*, 6682–6689.
(19) Huebner, A.; Srisa-Art, M.; Holt, D.; Abell, C.; Hollfelder, F.; deMello, A. J.; Edel, J. B. *Chem. Commun.* **2007**, 1218–1220.
(20) Berg, T. *Angew. Chem., Int. Ed.* **2005**, *44*, 5008–5011.
(21) Hodder, P.; Mull, R.; Cassaday, J.; Berry, K.; Strulovici, B. *J. Biomol. Screen.* **2004**, *9*, 417–426.
(22) Zaman, G. J. R.; de Roos, J. A. D. M.; Blomenrohr, M.; van Koppen, C. J.; Oosterom, J. *Drug Discovery Today* **2007**, *12*, 521–526.
(23) Leemhuis, H.; Stein, V.; Griffiths, A. D.; Hollfelder, F. *Curr. Opin. Struct. Biol.* **2005**, *15*, 472–478.

10.1021/ac800338z CCC: $40.75
Published on Web 04/10/2008

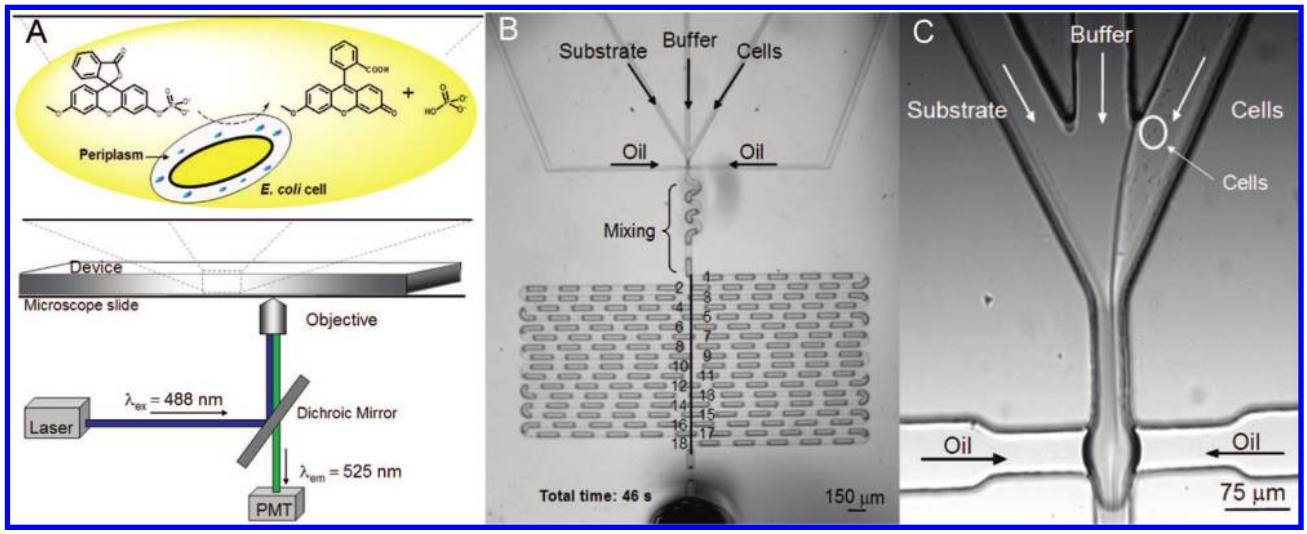

Figure 1. Scheme of the enzymatic reaction and the microfluidic device. (A) Assay of alkaline phosphatase produced in cells inside aqueous droplets in a mineral oil continuous phase. *E. coli* cells expressed alkaline phosphatase, which was exported into the periplasm. After encapsulation of cells in droplets with substrate 3-*O*-methylfluorescein-phosphate, the substrate diffused into the periplasm and was enzymatically hydrolyzed, generating a fluorescent product which was detected at 18 positions using a photomultiplier tube (PMT). (B) Droplet formation occurred by confluence of three aqueous inlet streams (substrate, buffer and cells) that were then intersected by two perpendicular oil streams [shown in detail in (C)]. Substrate concentrations were varied by changing the flow rates of substrate vs buffer solutions, keeping their combined flow rate equal to 15 μL/h. The flow rate of the cell feed was always kept constant at 5 μL/h. The numbers above the incubation loop (B) indicate various positions, corresponding to different times for the kinetic measurements. The images in (B) and (C) were taken with a Phantom V7.2 camera at 1000 frames per second with 2× and 60× magnification, respectively.

droplets were polydisperse (0.5 to 4.0 μm),[26] no doubt reducing the stringency of the selection.

It has been demonstrated that it is possible to encapsulate cells in water-in-oil microdroplets in microfluidic systems.[19,27,28] A cell-based enzymatic assay has been carried out detecting product in a single stationary droplet.[27] In this paper we describe experiments where multiple cell-based enzymatic reactions catalyzed by alkaline phosphatase (AP) are followed in individual, homogeneous droplets. Each droplet typically contains fewer than ten cells, and it is generated in a continuous process in a microfluidic device. In *Escherichia coli*, AP is exported to and concentrated in the cell periplasm, where it is more accessible to added hydrophilic or charged substrates than intracellular enzyme.[29] AP was used as a model enzyme as it is representative of a large class of hydrolytic enzymes employed in fine chemical synthesis and biotechnology, ranging from esterases[30–32] to phosphotriesterases.[33]

EXPERIMENTAL SECTION

DNA Expression Constructs. The gene for alkaline phosphatase with its native leader peptide was amplified by PCR from the plasmid pEK48[34] using oligonucleotides that introduced *Nde*I and *Hin*dIII restrictions sites (5′-GGAATTCCATATGAAACAAAG-CACTATTGCACTGGC-3′ and 5′-CTGAAATAAGCTTGCGCCCG-GCAGTGAAT-3′). The purified DNA was digested and ligated into the plasmid pET22b(+) (Novagen). The ligation mixture was used to transform *E. coli* BL21(DE3). DNA sequencing (Department of Biochemistry, University of Cambridge) of plasmid DNA (QIAGEN, QIAprep Spin Miniprep Kit) confirmed the correct sequence for the alkaline phosphatase gene. The mutant R166S was prepared by mutagenic plasmid amplification[35] with the following primer and its complement: CATGTGACCTCGTC-CAAATGCTACGGTC.

Cell Preparation. A cell culture was prepared by inoculation of fresh Luria−Bertani broth (LB, 4.0 mL) containing ampicillin (200 μg/mL) with 40 μL of an overnight culture of *E. coli* BL21(DE3) transformed with the plasmid harboring the gene for alkaline phosphatase. The culture was grown at 37 °C until the A_{600} reached ~0.55, and then the growth culture was cooled to 25 °C and induced with IPTG (0.025 mM final concentration) for ~14 h. An aliquot (1 mL) of the cell culture was centrifuged (3000*g*, 10 min) and the LB supernatant discarded. The cell pellet was resuspended (1 mL of fresh LB) and centrifuged under the same conditions. This procedure was repeated four times using mixtures with an increasing percentage (20 to 90%) of morpholine propane sulfonic acid (MOPS) buffer (100 mM MOPS pH 7.9; 100 μM $MgCl_2$ 10 μM $ZnSO_4$) in LB for resuspension. Finally, the cells were resuspended in MOPS buffer with 50% Percoll (Sigma-Aldrich) and diluted to an A_{600} of 1.0. Percoll is a silica particle suspension that minimizes cell sedimentation and facili-

(24) Aharoni, A.; Amitai, G.; Bernath, K.; Magdassi, S.; Tawfik, D. S. *Chem. Biol.* **2005**, *12*, 1281–1289.
(25) Mastrobattista, E.; Taly, V.; Chanudet, E.; Treacy, P.; Kelly, B. T.; Griffiths, A. D. *Chem. Biol.* **2005**, *12*, 1291–1300.
(26) Miller, O. J.; Bernath, K.; Agresti, J. J.; Amitai, G.; Kelly, B. T.; Mastrobattista, E.; Taly, V.; Magdassi, S.; Tawfik, D. S.; Griffiths, A. D. *Nat. Methods* **2006**, *3*, 561–570.
(27) He, M.; Edgar, J. S.; Jeffries, G. D.; Lorenz, R. M.; Shelby, J. P.; Chiu, D. T. *Anal. Chem.* **2005**, *77*, 1539–1544.
(28) Funfak, A.; Brosing, A.; Brand, M.; Kohler, J. M. *Lab Chip* **2007**, *7*, 1132–1138.
(29) Nikaido, H. *Microbiol. Mol. Biol. Rev.* **2003**, *67*, 593–656.
(30) Bottcher, D.; Bornscheuer, U. T. *Nat. Protocols* **2006**, *1*, 2340–2343.
(31) Bornscheuer, U. T.; Ordonez, G. R.; Hidalgo, A.; Gollin, A.; Lyon, J.; Hitchman, T. S.; Weiner, D. P. *J. Mol. Catal. B: Enzymatic* **2005**, *36*, 8–13.
(32) Morley, K. L.; Magloire, V. P.; Guerard, C.; Kazlauskas, R. J. *Tetrahedron: Asymmetry* **2004**, *15*, 3005–3009.
(33) Ghanem, E.; Raushel, F. M. *Toxicol. Appl. Pharmacol.* **2005**, *207*, 459–470.
(34) Chaidaroglou, A.; Brezinski, D. J.; Middleton, S. A.; Kantrowitz, E. R. *Biochemistry* **1988**, *27*, 8338–8343.
(35) Georgescu, R.; Bandara, G.; Sun, L. In *Directed Evolution Library Creation*; Arnold, F. H., Georgiou, G., Eds.; Humana Press Inc.: Totowa, NJ, 2003; Vol. 231, pp 75−83.

tates an even supply of cells to the microdevice over several hours. The final cell suspension was filtered (Minisart 5 μm, Sartorius) and used immediately.

Microfluidic Device Fabrication. The microfluidic device used in this study was fabricated from poly(dimethyl)siloxane (PDMS)[36,37] using standard soft lithographic methods.[38] Briefly, the devices were first designed with Autocad 2007 (Autodesk), and a dark-field mask was printed (Circuitgraphics). SU-8 2025 photoresist (MicroChem) was spin-coated onto a silicon wafer (diameter: 76.2 mm, Compart Technology Ltd.) at 500 rpm for 5 s and then ramped to 1000 rpm at an acceleration of 300 rpm/s for 33 s. This gave a final film thickness of 75 μm, as measured by profilometry on the finished master (DekTak 150). After spinning, the wafer was prebaked (3 min at 65 °C, then 9 min at 95 °C and finally 3 min at 65 °C), and then exposed to UV light through the mask on a mask aligner (MJB4, Suss Microtech). After postbaking and development, the master was hard-baked for 1 min at 170 °C. A 10/1 (w/w) ratio of poly(dimethyl)siloxane (PDMS) and curing agent (Sylgard 184) was poured over the master, degassed and then baked overnight at 75 °C. The devices were cut and peeled off the master. Access holes for the inlet tubes were punched using a biopsy punch. The device was then exposed to an air plasma for 30 s (Diener Femto plasma asher), sealed to a glass microscope slide, and baked overnight at 75 °C.

Operation of the Device. Syringes (Hamilton, Gastight, 100 μL) were connected *via* polyethylene tubing (Intramedic, i.d. 0.38 mm) to the device. Flow control was achieved with the use of syringe infusion pumps (Harvard Apparatus 2000). Mineral oil was used as the continuous phase (Sigma-Aldrich) with 1.5% (w/w) AbilEm90 (Goldschmidt GmbH, Essen/Germany) as a surfactant.[1] This mixture formed droplets that did not subsequently cause wetting in the device, which is a common problem with other oil/surfactant mixtures.

The size, frequency and speed of the droplets within the device were regulated by controlling the flow rate of the aqueous solutions and the total oil flow. For all the experiments described in this work, the sum of the flow rate in the three aqueous streams was 20 μL/h and the total oil flow rate was 20 L/h. All liquids (apart from the cell solution) were filtered using a 0.22 μm filter cartridge (MillexGP, 0.22 m, Millipore) and degassed before being fed into the chip. All experiments were conducted at 24 °C. The size of the droplets was estimated to be the same as the width (75 μm) and depth (75 μm) of the microchannel.

Detection Systems. A Phantom V72 camera recorded pictures at 1000 frames per second in bright-field mode and was used to calculate the droplets' transit time in the device (A video was deposited at http://www-microdroplets.ch.cam.ac.uk/research/movies.html). To visualize fluorescent cells within a droplet an EMCCD camera (XonEM$^+$ DU 897, Andor) was coupled to a microscope (Olympus IX71) with the device illuminated with a 100 W mercury arc lamp (Olympus U-RFL-T). For the high-throughput analysis of the fluorescent cells and the kinetic measurements the microfluidic device was placed on the microscope and coupled to a diode-pumped solid state laser excitation source (Piccaro 488 nm air-cooled cyan). A 10× microscope objective (UPlanFLN, Olympus) was used to focus the light within the microfluidic channel. Fluorescence emitted by the sample was collected by the same objective and transmitted through a dichroic mirror. A filter cube (UMWIB, Olympus) was used to remove any residual excitation light.

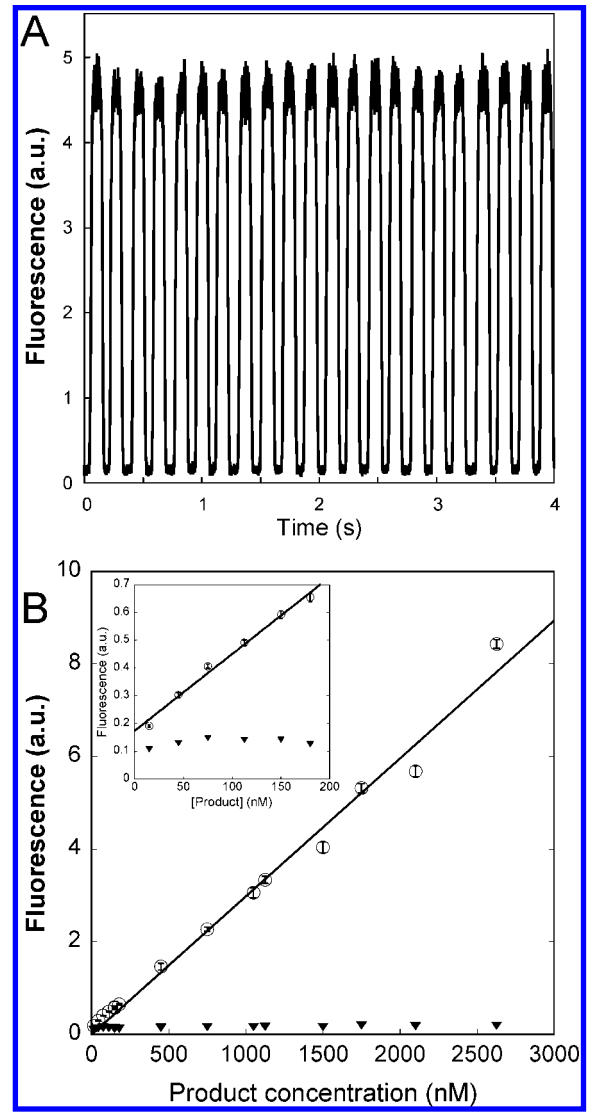

Figure 2. Fluorescence detection in each droplet. (A) Data trace of product fluorescence (1.75 μM, OMF) obtained by laser detection and displayed with LabView. (B) Variation of product concentration vs fluorescence (peak height) gives a linear relationship between 12 nM and 2.6 μM. Standard deviations are indicated by error bars. The inset in (B) shows this relationship at low product concentrations (12−180 nM). In both graphs the filled triangles (▼) represent the background signal. The curve in Figure 2B was generated by changing the relative flow rates of the buffer and product inlets, keeping the total flow of the aqueous solution constant at 20 μL/h. The droplets contained buffer and cells without the expression plasmid for alkaline phosphatase. Conditions: [MOPS] = 100 mM, pH 7.9, 24 °C.

Analysis of Droplet Fluorescence. The voltage readout of the photomultiplier tube (PMT, H8249, Hamamatsu Photonics) was recorded and fed into a computer by a data acquisition card (DAQ, PCI 6251, National Instruments) and processed using LabView 8.2 (National Instruments). To determine the height of the fluorescent peaks, the data was first frequency filtered to reduce the effect of noise before being processed by the in-built

(36) Duffy, D. C.; McDonald, J. C.; Schueller, O. J. A.; Whitesides, G. M. *Anal. Chem.* **1998**, *70*, 4974–4984.
(37) Whitesides, G. M. *Annu. Rev. Mater. Res.* **1998**, *28*, 153–184.
(38) McDonald, J. C.; Duffy, D. C.; Anderson, J. R.; Chiu, D. T.; Wu, H.; Schueller, O. J.; Whitesides, G. M. *Electrophoresis* **2000**, *21*, 27–40.

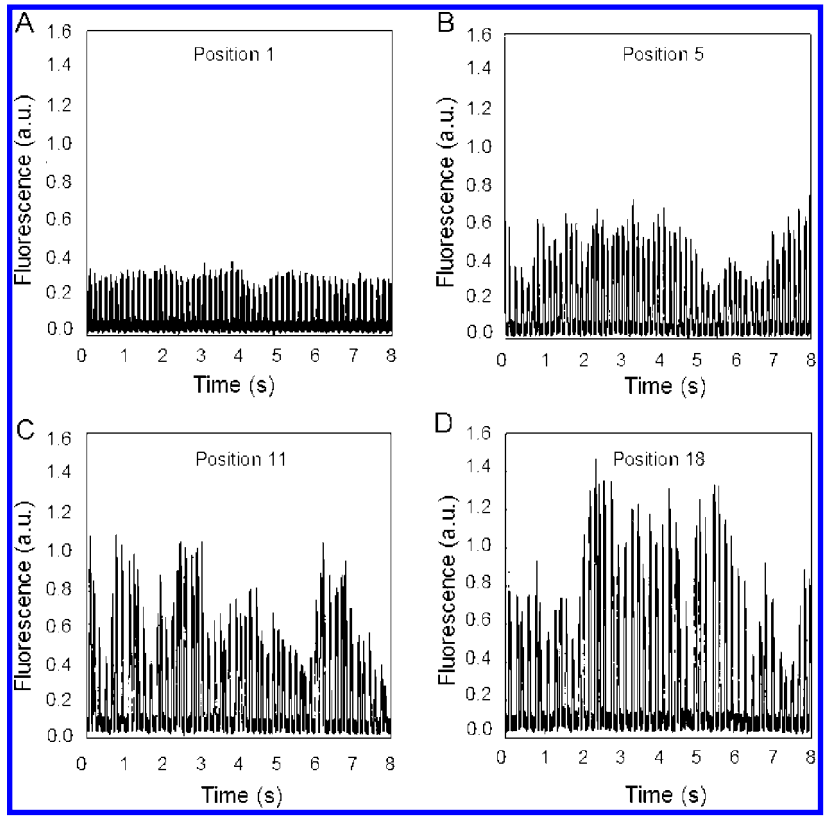

Figure 3. Data traces showing the laser-induced fluorescence from droplets detected along the reaction channel (see Figure 1B) at position 1 (A, $t = 0.74$ s), position 5 (B, $t = 11.4$ s), position 11 (C, $t = 27.3$ s) and position 18 (D, $t = 46$ s). Increasing residence times in the device led to higher average fluorescence (see Figure 5C), indicating that more product had been generated. There was also a greater spread in the fluorescence detected in individual droplets, due to different numbers of cells in different droplets. Conditions: [S] = 50 μM, pH 7.9, $T = 24$ °C.

Table 1. Distribution of Peak Heights of Droplets Containing Substrate and *E. coli* Cells Periplasmically Expressing Alkaline Phosphatase[a]

position	time (s)	mean fluorescence (a.u.)	STDV	coefficient of variance (STDV/mean) × 100
1	0.7	0.24	0.03	11.1
5	11.4	0.38	0.14	36.2
11	27.3	0.53	0.21	39.6
18	46.0	0.73	0.30	41.2

[a] Shown here are the mean, standard deviation (STDV) and coefficient of variance (CV) values of a population of droplets measured at different positions in the device corresponding to different time points.

peak detection algorithm. A region of interest is used to discriminate against background noise. The heights for each time point were averaged and the standard deviation and the coefficient of variance were calculated.

RESULTS

The experimental scheme is shown in Figure 1. *E. coli* cells expressing the enzyme alkaline phosphatase were encapsulated in droplets in a microfluidic device with the fluorogenic substrate 3-*O*-methylfluorescein phosphate (OMFP). The alkaline phosphatase was exported to the cell periplasm where it concentrated, and catalyzed the dephosphorylation of substrate to generate the fluorescent product 3-*O*-methylfluorescein (OMF).[29] The laser-induced fluorescence of this product was monitored *via* the signal detected in a photomultiplier (PMT).

Device Design. Droplet formation was achieved using a flow focusing geometry using three aqueous inlet channels[39,40] that cocompartmentalized the substrate OMFP, buffer, and *E. coli* cells harboring alkaline phosphatase (Figure 1A). The typical droplet volume was ~840 pL, and the speed of droplet formation was approximately 6 Hz. After droplet formation a short "wiggle" module allowed rapid mixing of droplets by chaotic advection within less than 1 s.[14] The droplets then flowed through a long channel in which fluorescent product was quantified at 18 positions (see Figure 1B) corresponding to 18 reaction times. The total transit time of an individual droplet moving from position 1 to 18 is approximately 46 s. At each position, we measured the fluorescence of >1000 droplets.

Droplet Characterization. Initial experiments were carried out to characterize the polydispersity of the droplets and establish the limits of the fluorescence detection of the system used. To this end, droplets were generated containing only buffer, predefined concentrations of the fluorescent product (OMF) and cells lacking the expression plasmid or alkaline phosphatase. The cells were included so that the viscosity at the point of droplet formation would match that in subsequent kinetic experiments. A typical data trace of fluorescence measured over time at the last detection point (position 18) is

(39) Anna, S. L.; Bontoux, N.; Stone, H. A. *Appl. Phys. Lett.* **2003**, *82*, 364–366.
(40) Ward, T.; Faivre, M.; Abkarian, M.; Stone, H. A. *Electrophoresis* **2005**, *26*, 3716–3724.

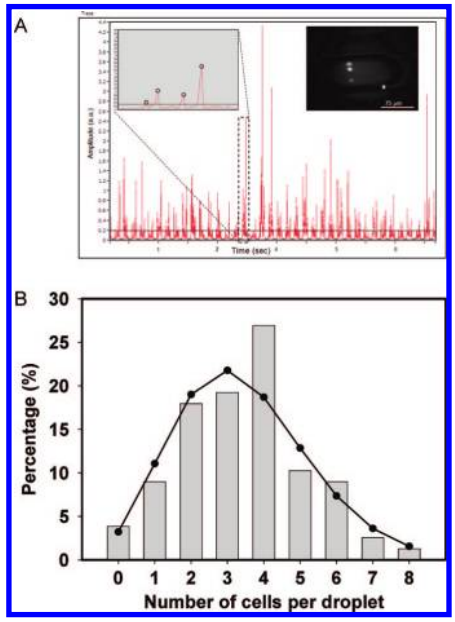

Figure 4. Cell distribution within droplets. (A) The mainframe shows the data trace of encapsulated cells that expressed green fluorescent protein (GFP). The inset on the top left shows a zoom into one droplet. Varying peak heights indicate the phenotypic variation of GFP expression levels of different cells. The gray bar horizontally to the *x*-axis indicates the threshold set for detection of cells. The other inset (upper right) shows encapsulated cells, expressing the green fluorescent protein within the device. The picture was taken with an Andor XonEM$^+$ DU 897 EMCCD camera. (B) Distribution of number of cells per droplet (gray bars) compared to a Poisson distribution (filled circles).

shown in Figure 2A. Peak heights were recorded and used to characterize the fluorescence in each droplet. The fluorescent signal was found to be linearly dependent on product concentration between 12 nM and 2.6 μM (Figure 2B). For each concentration the peak heights were uniform with a typical coefficient of variance (standard deviation/mean $\times$ 100) of 3%, consistent with the low polydispersity of droplet size observed in images of the droplets.

Monitoring the Reaction Progress. Figure 3 shows typical data traces for product formation when cells expressing AP and substrate were cocompartmentalized. The increase of fluorescence was measured at different positions along the reaction channel corresponding to reaction times up to 46 s (in positions 1−18, Figure 1B). The wiggle channel before position 1 corresponds to a dead time of 0.74 s. While initially the peak heights were relatively homogeneous with a coefficient of variance (CV) of 11% (Figure 3A), a progressively greater spread of peak heights up to 41% at position 18, coupled with an increase in the average level of fluorescence intensity, was observed as the droplets traveled further through the device (see Figures 3B−D and Table 1).

The increasing distribution of peak heights is further analyzed below and is likely to be due to varying numbers of cells in different droplets, giving rise to varying enzyme concentrations or to phenotypic variation in expression levels. To estimate how many cells were encapsulated per droplet, cells expressing the green fluorescent protein (GFP) were monitored with an epifluorescence laser system setup. It is clear from the fluorescent trace shown in Figure 4A and the inset showing encapsulated cells that our system easily allows us to "spatially resolve" the fluorescence from individual droplets. We were therefore able to count the number of cells in each droplet by following the number of fluorescence bursts per droplet. Counting the cell load for hundreds of droplets led to a cell distribution between 0 and 8 cells (see Figure 4B). The distribution of cells per droplet is in good agreement with the results that we have published recently.[19]

The distribution of the number of cells per droplet follows a Poisson distribution. Figure 4B shows the measured number of cells per droplet and the corresponding Poisson distribution, which is defined by

$$y(k) = \frac{\lambda^k e^{-\lambda}}{k!}$$

where k is the number of cells per droplet and λ is the mean number of cells per droplet. This distribution is also similar to

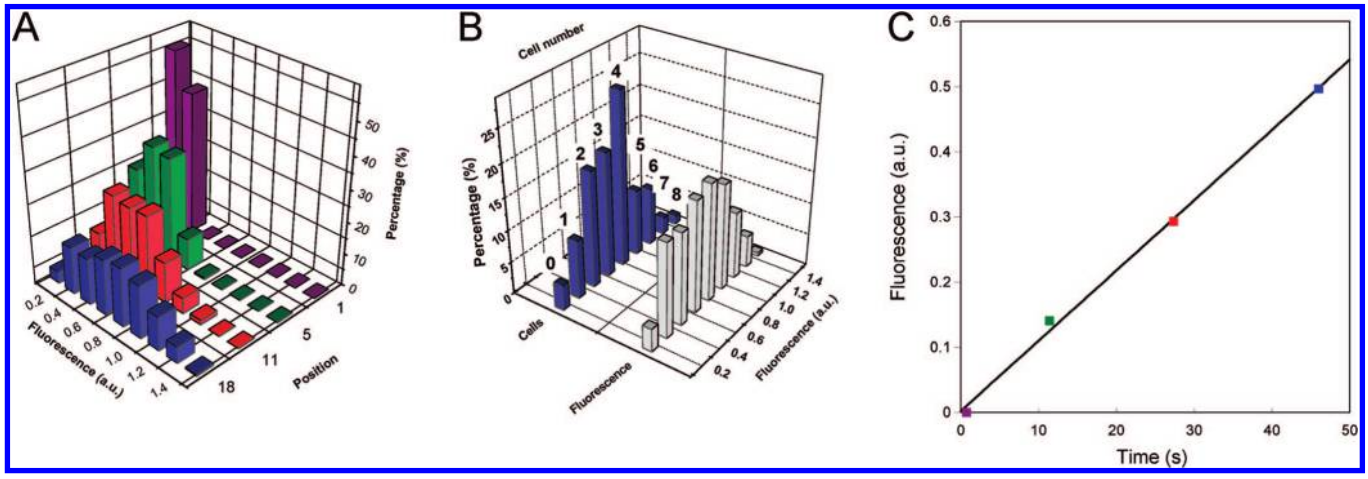

Figure 5. Analysis of droplet occupancy. (A) The fluorescence distribution in droplets at position 1 (t = 0.74 s), position 5 (t = 11.3 s), position 11 (C, t = 27.3 s) and position 18 (t = 46 s) presented as a nine bin histogram. (B) The spread in the measured fluorescence of individual droplets at position 18 was compared to the distribution of cells expressing GFP per droplet (as in Figure 4B) under the same conditions. Approximately 4% of the droplets at position 18 show no increase in fluorescence and are assumed to be empty. (C) Linear graph obtained when the average fluorescence intensities of >1000 droplets from each time point were plotted. The coloration corresponds to the data in panel A that also indicates the spread of fluorescence intensity as a consequence of occupancy. The data were corrected for the background signal. Conditions: [S] = 50 μM, pH 7.9, T = 24 °C.

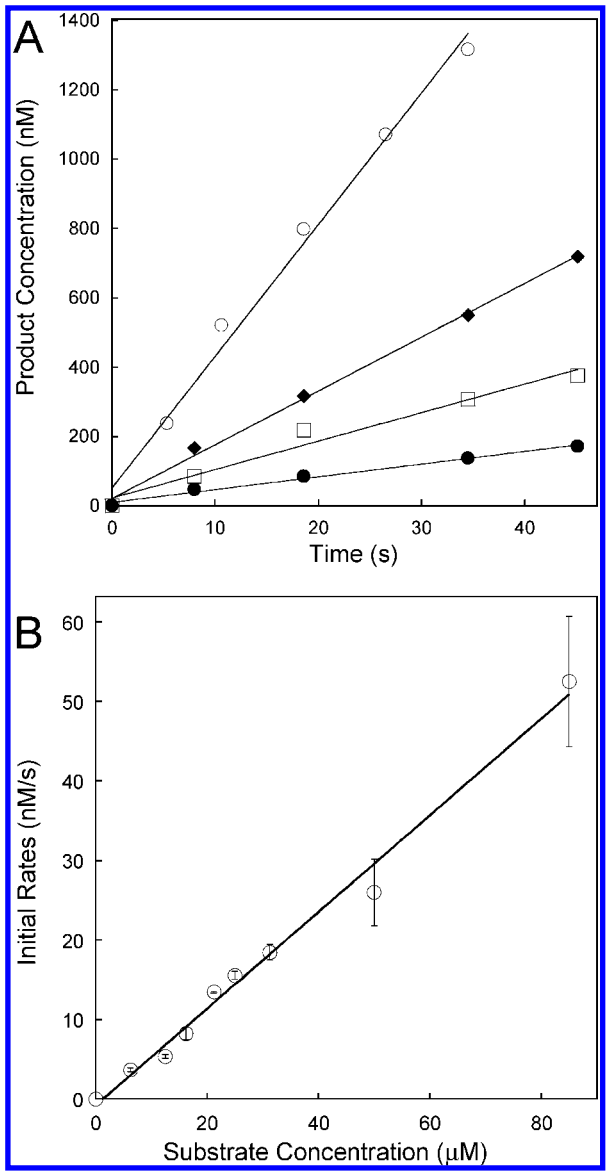

Figure 6. (A) Kinetic traces obtained for different substrate concentrations (● 6.25 μM; □ 16.25 μM; ◆ 25.00 μM and ○ 50.00 μM). Each point represents the average intensity of >1000 droplets measured individually in five different positions along the channel. (B) Dependence of initial rate vs initial substrate concentration. Initial rates were derived from linear least-squares fits of the time courses in panel A (with error bars arising from the fit). Conditions: pH 7.9, T = 24 °C.

the distribution of product fluorescence seen at position 18 in the device (Figure 5B). This similarity of distributions supports the hypothesis that the source of heterogeneity in peak heights results from the variation in the number of cells per droplet. In the future AP labeled with a fluorescent marker could be used to correlate the activity in each droplet with the number of cells and the amount of protein. The fluorescence data on the GFP-producing cells show that we can reliably investigate fluorescence signals from droplets containing single cells. Although we did not pursue this goal in this work, dilution experiments could be carried out to ensure a maximum of one cell per droplet.[19]

The heterogeneity in cell distribution per droplet and the corresponding variation in the amount of enzyme produced and consequently product formed in different droplets are randomly

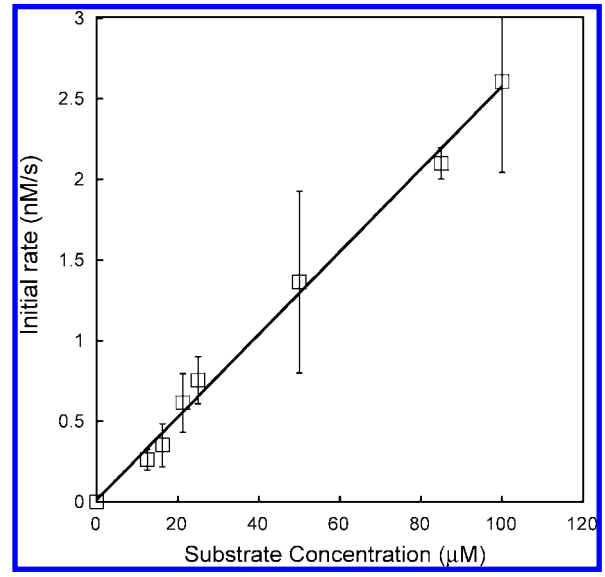

Figure 7. Initial rates of alkaline phosphatase mutant R166S. The rates were obtained from linear least-squares fits of time courses as in Figure 6A (and are displayed with error bars arising from these fits). The linear increases of initial rates with substrate for this mutant are 24-fold lower than for wild type. This reflects the 30-fold difference in k_{cat}/K_M between wild type and mutant.[34] Conditions: pH 7.9, T = 24 °C.

distributed. Under the conditions of the experiment any 1000 droplets will contain on average the same number of cells, and it is therefore possible to follow the overall rate of reaction at any time point by counting sufficient droplets and taking the average. Therefore the increase in fluorescence can be attributed to an average increase per cell.

This is demonstrated in Figure 5C. The linear increase of the fluorescence intensity with time can be plotted from the measurement of peak height averaged over >1000 droplets.

Measuring Reaction Rates at Different Substrate Concentrations. To characterize the kinetic properties of the enzyme it is necessary to carry out a series of experiments where the rate of reaction is monitored as a function of substrate concentration. This analysis can yield steady state kinetic parameters and would normally be expected to show saturation kinetics with a maximum rate. Using the microfluidic device the substrate concentration was varied by altering the flow rate of the substrate stream, with compensating adjustment of the buffer stream, keeping the combined flow rates constant. The flow rate of the third stream, delivering the cell suspension, was held constant throughout so that the same average number of cells were dispensed throughout all experiments. Figure 6A shows kinetic traces from measurements at five different positions in the channel using different substrate concentration. For each point the average fluorescence over 1000 droplets was recorded. Initial rates were calculated from these traces, and the slopes were plotted against substrate concentration (Figure 6B). The homogeneity of the droplets results in reproducible data that gave well-defined initial rates with small fitting errors (Figure 6B). Strikingly, there is no evidence of saturation kinetics, even though the maximum substrate concentration is over 10-fold higher than the K_M (6.0 μM) determined for the purified enzyme in bulk solution.

This result was expected, as a similar observation has been reported by Martinez et al. for the hydrolysis of 4-nitrophenyl

phosphate by alkaline phosphatase expressed in the periplasm of *E. coli,* measured using cuvettes in a spectrophotometer.[41,42] The lack of saturation kinetics was ascribed to a much lower substrate concentration in the periplasm compared to bulk solution, due to the outer membrane barrier.[41,42] Another possible explanation could be rate limiting diffusion of substrate to the enzyme in the periplasm.

In order to investigate the reason for the lack of saturation kinetics, the enzymatic activity of *E. coli* cells expressing the alkaline phosphatase mutant R166S was investigated. Compared to wild type, this enzyme has been shown to have a 30-fold lower k_{cat} but a similar K_M value and similar expression levels.[34] The kinetic experiments were repeated in droplets using *E. coli* expressing the mutant protein. Figure 7 shows the initial rates obtained from kinetic traces (corresponding to those in Figure 6A for the wild type enzyme). Again there is no evidence for saturation kinetics, the slope corresponding to a second order rate constant 24-fold lower than that measured for the wild type enzyme. The observation of a reduced activity for the mutant is not consistent with rate limiting transport of substrate or product across the periplasm, and supports the interpretation of Martinez et al. that the periplasmic concentration of substrate is low relative to K_M.

CONCLUSIONS

These experiments demonstrate that it is possible to assay individual enzyme reactions confined to picoliter volumes in aqueous microdroplets. The enzyme studied was expressed in the periplasm of *E. coli* cells encapsulated in the droplets, and the enzymatic activities measured were in good agreement with larger scale low throughput assays. Assaying periplasmically expressed enzymes has the advantage that the enzyme concentration locally builds up so rapid turnover can be observed allowing quick assays to be performed. Furthermore, substrate can easily reach the enzyme, which would not necessarily be the case if it were expressed intracellularly. Alkaline phosphatase has a leader peptide sequence that naturally leads to its export to the periplasm. In principle similar sequences could be genetically appended to many other enzymes, allowing them to be assayed in a similar way. As well as being an example of a study of a periplasmic enzyme, the system described could also be used as part of a screen to identify inhibition of protein export, either by small molecules introduced into the droplets or by genetic lesion in *E. coli* by screening a library of mutants.

Microdroplets share the attributes of a laboratory-on-a-chip process, using small amounts of reagents that are precisely dispensed into droplets and additionally offer a number of advantages compared to other cell based assays. Assays with whole cells carried out in well plates consume μL to mL of reagents, and their overall throughput is limited.[43,44] Cell colony assays on agar plates are effectively end point assays and depend upon having a product that precipitates. Assays in microdroplets can provide more detailed kinetic data and potentially a higher throughput than either of these techniques.

The experiments reported here exhibit a significant advance on previously reported kinetic studies on enzyme reactions in microdroplets where either the average fluorescence of a droplet stream was measured[14] or the fluorescence of one stationary droplet was recorded.[27] The sensitivity of laser induced fluorescence has previously enabled detection of encapsulated cells at high speed arrangement.[19] Here this technique was applied to measure the enzymatic activity in a single droplet of very few cells, allowing discrimination between droplets containing differing numbers of cells. The technique has the potential to detect enzyme activity from single cells, and to discriminate between cells expressing enzymes with different activities. Coupled with sorting tools of the type recently described,[6,10] this technique will become a useful tool for directed evolution studies, to characterize and select improved enzyme variants from protein libraries.

(41) Martinez, M. B.; Flickinger, M. C.; Nelsestuen, G. L. *J. Biotechnol.* **1999**, *71*, 59–66.
(42) Martinez, M. B.; Schendel, F. J.; Flickinger, M. C.; Nelsestuen, G. L. *Biochemistry* **1992**, *31*, 11500–11509.
(43) Allen, M. D.; DiPilato, L. M.; Rahdar, M.; Ren, Y. R.; Chong, C.; Liu, J. O.; Zhang, *ACS Chem. Biol* **2006**, *1*, 371–376.
(44) Inglese, J.; Johnson, R. L.; Simeonov, A.; Xia, M.; Zheng, W.; Austin, C. P.; Auld, D. S. *Nat. Chem. Biol.* **2007**, *3*, 466–479.

ACKNOWLEDGMENT

This work was supported by the RCUK Basic Technology Programme. A.H. was supported by a studentship of the EU Early-Stage Research Training Site ChemBioCam. F.H. is an ERC Starting Investigator. We thank Prof. D. Weitz (Harvard) for initial help with the design and operation of microfluidic devices.

Received for review February 18, 2008. Accepted March 7, 2008.

AC800338Z